TJ *et al.*
Future Journal of Pharmaceutical Sciences (2023) 9:121
https://doi.org/10.1186/s43094-023-00566-1

Future Journal of Pharmaceutical Sciences

RESEARCH Open Access

Nano-calcium incorporated piscean collagen scaffolds: potential wound dressing material

Chaitra Shree TJ[1], Sindhu Abraham[1*], Sharon Furtado[1], Darshan Ramesh[1], Kesha Desai[2] and Bharath Srinivasan[1]

Abstract

Background Collagen proteins extracted from piscean sources are alternatives to bovine and porcine collagen because of their abundance, low price, and skin compatibility and are being explored as suitable wound dressing materials. Intracellular calcium ions are crucial for wound healing, and studies have shown that calcium ion supplementation via an external medium is equally beneficial for speedy recovery. This study explores the wound healing potential of dressing materials that encompass the benefits of nano-calcium and piscean collagen. Nano-calcium sulphate (NCS)-integrated scaffolds were prepared with 100 ppm of NCS and varying concentrations of piscean collagen and HPMC E15 LV. The thickness, tensile strength, folding endurance, pH, expansion profile, and moisture vapour transmission properties of the scaffolds were determined. An in vitro scratch assay and an excision rat wound model were employed to evaluate the wound healing properties of the scaffolds.

Results The NCS particles had a mean particle size of 220.7 nm. The scaffolds demonstrated an acceptable thickness, mechanical strength, and flexibility. The scratch assay results revealed that at the end of 24 h of the study, there was an increased wound closure rate with collagen scaffolds in contrast to the control group. In the vivo wound healing studies, formulation CS6 showed 100.0% healing on day 12 as compared to other formulations.

Conclusions Wounds treated with scaffolds contracted faster than those treated with a commercial collagen dressing and the control group. The current study thus demonstrates the wound healing ability of nano-calcium sulphate-incorporated piscean collagen scaffolds.

Keywords Nano-calcium, Scaffold, Cytocompatibility, Scratch assay, Piscean collagen

Background and introduction

Wound treatment is often considered to be a daunting task, although there is an assortment of dressings with various functionalities. Traditional wound treatment methods mainly attempt to control bleeding and infection, whereas wound dressings modify the wound environment into a microenvironment that is similar to an acute wound, allowing it to heal naturally [1–4]. To promote effective healing, a wound dressing material that is easy to use and provides a favourable environment with properties such as maintaining a balanced moisture level, tissue compatibility, and protection from infection and contamination is ideal [5]. To promote a healing environment, collagen biomaterials stimulate angiogenesis and fibroblast deposition and enhance the metabolic activity of granulation tissue. Collagen scaffolds can be utilized for both acute and chronic wounds and provide excellent

*Correspondence:
Sindhu Abraham
sindhu.ps.ph@msruas.ac.in
[1] Department of Pharmaceutics, Faculty of Pharmacy, M S Ramaiah University of Applied Sciences, Gnanagangothri Campus, Bengaluru, India
[2] Department of Pharmacology, Faculty of Pharmacy, M S Ramaiah University of Applied Sciences, Gnanagangothri Campus, Bengaluru, India

mechanical support to minimize oedema in the injured area [6–9]. Although collagen dressings are ideal for wounds and severe burns, the price remains a deterrent. Additionally, collagen may provide an excellent milieu for bacterial growth, causing exudation and delayed healing [10].

Piscean collagen has garnered significant interest due to its ample supply, affordable cost, and excellent compatibility with human skin [11]. When compared to bovine or porcine collagen, there are no limitations regarding the use of piscean collagen for any religion, and there are no reported risks of disease transmission [12–15].

Calcium plays a critical role in the sequential stages of the wound healing process. Studies performed on various model organisms have shown that both intracellular and extracellular Ca^{2+} are equally important for healing [16, 17]. This understanding has paved the way for the use of calcium-incorporated wound dressings [18]. The hemihydrate form of calcium sulphate is used extensively as osteoconductive scaffolds for the regeneration of bone tissue and for guided regeneration of periodontal tissue in dentistry [19, 20]. Studies have provided evidence that calcium sulphate and extracellular cell matrix membrane in combination produce synergistic effects on bone regeneration as a result of angiogenesis being stimulated in the preliminary phases of healing [21–23]. Walsh et al. [24] investigated the impact of calcium sulphate dissolution on the pH of the local environment in bone-grafted areas and concluded that upon dissociation, the release of calcium ions causes a drop in the local pH, resulting in antimicrobial action and improved wound healing. Nano-calcium sulphate (nano-$CaSO_4$), a form of calcium sulphate engineered into nanoparticles, has unique properties such as a high surface area-to-volume ratio, which can potentially enhance their interactions with cells and tissues. Park et al. [25] demonstrated that nano-calcium sulphate particles (< 100 nm) had a better attachment to osteoblastic cells, followed by growth and differentiation. Nano-$CaSO_4$ when incorporated into wound dressings or gels can help prevent or control bacterial infections, which normally impede the healing process. This can be attributed to its increased surface area, ability to control degradation rate, and drug release. Calcium sulphate, if present in nano-form, will therefore have a higher surface area, leading to improved bioavailability on application [26, 27].

This study aimed to evaluate the wound healing benefits of scaffolds prepared with piscean collagen and loaded with nano-calcium sulphate, using in vitro and in vivo models. The incorporation of calcium sulphate into collagen scaffolds has several potential benefits for wound healing. These scaffolds provide a framework that mimics the extracellular and promotes cell attachment, migration, and proliferation. The incorporation of calcium sulphate further enhances the structural integrity of the scaffold, providing mechanical support to the wound site. While calcium ions are crucial for cell signalling, adhesion, and migration to facilitate tissue repair, sulphate ions can trigger the production of glycosaminoglycans and proteoglycans, which are indispensable components of the extracellular matrix [28]. Nano-calcium sulphate not only encourages healing but also mitigates any associated infections. The combination of calcium sulphate and piscean collagen results in a unique biomaterial that offers several benefits for wound healing, including enhanced tissue regeneration, antimicrobial properties, and improved mechanical strength. The film-forming and shape-retaining properties of the scaffold were modified with the incorporation of HPMC E15LV [29, 30]. Glycerol was incorporated to enhance the mechanical characteristics and flexibility of the scaffold.

Methods

Materials

Piscean collagen was sourced from Himrishi Herbals in India. Yarrow Chem Products in India supplied HPMC E15LV and calcium sulphate. Calcium carbonate, nitric acid, and glycerol were obtained from Rankem, India. Culture media for sterility testing was purchased from Sigma-Aldrich, India. L929 murine fibroblast cell lines were procured from National Centre for Cell Science, Pune.

Nano-calcium sulphate (NCS): preparation and characterization

A 7% calcium sulphate solution was sonicated using a probe sonicator (QSONICA, CL-334, India) to create a uniform dispersion, which was then poured into Petri plates and dried in a tray dryer (Ti-130FAC, India). The particle size of the NCS was determined and then used in the preparation of the scaffold [20].

Size and distribution of NCS particles

The dispersion of NCS in deionized water was characterized for its particle size by dynamic light scattering (DLS) using a Zeta Potential & Particle Size Analyser (NanoBrook ZetaPALS, USA). The processed data were obtained using the ZetaPALS software (version 5.23).

Formulation of collagen scaffolds (CS)

The solvent casting method was employed to prepare the scaffolds. An NCS stock solution of 1000 ppm (parts per million) strength was prepared, from which a volume equivalent to 100 ppm of NCS was withdrawn and used in the preparation of scaffolds. Varying concentrations of collagen (5–15%) and HPMC E15LV (5–10%) were used

to obtain scaffolds with desired characteristics. The concentrations were determined based on preliminary trials. Glycerol (1.5%) was used as the plasticizer for all the formulations (Table 1). The scaffolds were vacuum-dried (Ti-136GW, Tempo, India) and kept in a desiccator for evaluation.

Evaluation of collagen scaffolds

Microscopic analysis and elemental composition

SEM–EDX analysis was performed on both NCS and NCS-loaded scaffolds using a Zeiss ULTRA 55 microscope (Germany). The samples were prepared by exposing them to gold vapours in an argon atmosphere and affixing them to the sample holder. The surface morphology and elemental composition were examined at 5 KX and 25 KX magnifications.

pH

The surface pH of each scaffold was measured by bringing the probe of a digital pH meter (MK-VI, Systronics, India), into close contact with the moistened scaffold. Measurements were carried out thrice, and the mean value was determined for comparison [31, 32].

Thickness, folding endurance, and mechanical properties

The time required for a scaffold to absorb wound exudates and form a barrier over a wound is influenced by its thickness. A screw gauge was used to measure the thickness at three different points on the scaffold, and the average of the three measurements was considered [31].

The flexibility required for the easy handling and application of scaffolds can be measured using a folding endurance test. The scaffolds were continually folded at a particular location until they were cut. The total number of folds that could be made without causing damage was considered folding endurance [33].

The mechanical properties of the scaffolds were evaluated utilizing a universal testing machine (MultiTest 10-I, UK). As per the ASTM D882-02 standards [34], scaffolds with dimensions of 30 mm × 10 mm were positioned between the tester grips and stretched. A minimum grip separation of 50 mm and cross-head separation speed of 50 mm/min were maintained uniform for all measurements. The machine was fitted with a load cell that could measure the maximum applied force. The tensile strength (MPa) and % elongation at break (% E) of the cut scaffolds were determined using the following formulae [27, 35]:

$$\text{Tensile strength(MPa)} = \frac{\text{Maximum force}(N)}{\text{Cross - sectional area}\left(\text{mm}^2\right)}$$

$$\%\, E = \frac{\text{Length at rupture} - \text{Initial length}}{\text{Initial length}} \times 100$$

Moisture vapour transmission rate (MVTR) studies

The permeation characteristics of the scaffolds were measured according to ASTM E96 testing guidelines [36]. One gram of anhydrous calcium chloride was placed inside dry glass vials and then sealed with a scaffold of diameter 1.5 cm. The vials were weighed and placed in an environmental chamber under controlled conditions of humidity (50 ± 2%) and temperature (32 °C) for 24 h. The vials were reweighed, and MVTR was calculated as follows:

$$\text{MVTR}\left(\text{g/m}^2\right)/24\text{h} = \frac{W}{S}$$

where W is the increase in the weight of calcium chloride at the end of 24 h (g), and S is the exposed surface area of the scaffold (m^2).

Expansion studies

Gelatin was used as a medium to simulate the moist environmental conditions of exuding wounds. Hot gelatin solution (4% w/v) was allowed to be set in Petri dishes by cooling (25 °C). A scaffold of diameter 22 mm (D_0) was positioned in the middle of the solidified gelatin. The increase in the diameter (D_t) of the scaffold on the absorption of moisture was measured at fixed time

Table 1 Composition of collagen scaffolds

Ingredients	Formulations					
	CS 1	CS 2	CS 3	CS 4	CS 5	CS 6
Nano-calcium sulphate (ppm)	100	100	100	100	100	100
Piscean collagen (g)	5	10	15	5	10	15
HPMC E15LV (g)	5	5	5	10	10	10
Glycerol (mL)	1.5	1.5	1.5	1.5	1.5	1.5
Purified water (q.s)	100 mL	100 mL	100 mL	100 mL	100 mL	100 mL

intervals [27, 33, 37, 38]. The test was repeated thrice to generate the average value for the calculation.

$$\text{Expansion ratio}(E) = \frac{D_t - D_0}{D_0} \times 100$$

Sterilization and sterility testing

The prepared scaffolds were sterilized using ultraviolet radiation at 254 nm for 2 h (for each side) and packaged in sterilized aluminium packaging [39]. Sterility testing was performed to validate the effectiveness of the sterilization process. Fluid thioglycollate medium was used to identify aerobes, anaerobes, and microaerophiles, post-incubation of scaffolds in medium at 30–35 °C for 14 days, while soyabean casein digest medium was used to identify fungi, after incubation at 20–25 °C for 14 days.

Cytocompatibility testing

The influence of collagen scaffolds on the metabolic activity of L929 murine fibroblast cell lines was assessed using an MTT assay [40]. This study involved the measurement of the colour intensity of formazan crystals (purple colour) formed by the reduction of MTT (yellow colour) by metabolically active cells. Fibroblasts were cultured, trypsinized, and aspirated into sterile centrifuge tubes. The cell density was adjusted using DMEM-HG medium and seeded into a 96-well microtiter plate with a cell mass of 10,000 cells (200 µL/well). The plate was incubated at 37 °C in a 5% CO_2 atmosphere for 24 h. Post-incubation, the medium was aspirated and replaced with 200 µL of sample (2.5% v/v). The plate was then incubated for 48 h under the same conditions, followed by media aspiration. 200 µL of media containing 10% MTT reagent was added to each well to create a mixture with a concentration of 500 µg/mL and incubated for 3 h. The insoluble crystals of formazan were solubilized in 100 µL of DMSO, and the absorbance was measured at 570 nm and 630 nm. The values were used to calculate cell viability:

$$\%\ \text{Cell viability} = \frac{\text{Absorbance (sample)} - \text{Absorbance (blank)}}{\text{Absorbance (control)} - \text{Absorbance (blank)}} \times 100$$

Acute dermal irritation studies

The potential for scaffolds to cause dermal irritation was evaluated in healthy female albino rabbits in compliance with OECD 404 guidelines for testing chemicals [41]. The Institutional Ethics Committee for animal research approved all animal study procedures. The animals were individually housed under controlled environmental conditions (20 ± 3 °C/50–60% RH) with 12-h light and 12-h dark cycle, maintained on a pellet diet, and unrestricted supply of drinking water. The fur on the dorsal area of the rabbits was carefully epilated 24 h before the test, and the rabbits were randomly distributed into groups of six, with one group for the control and the other for the formulation. Formulation CS 6 containing 15% of piscean collagen and 10% HPMC E15LV was subjected to testing. Approximately 6 cm^2 of the scaffold was kept in contact with the shaved area and secured with gauze. At the end of the contact period of 4 h, the scaffolds were gently removed, and all animals were examined for signs of erythema and oedema. The severity of erythema/oedema was graded on a scale of 0–4, where 0 indicated the absence of any signs of redness/swelling and 4 indicated the presence of severe redness/swelling. Grading was performed 60 min after patch removal and 24, 48, and 72 h later.

In vitro scratch assay

This study provides a practical and convenient approach for analysing cell migration, which is vital for the regeneration of injured tissues. A cell-free gap was created by scratching a monolayer of cell culture, and the movement of cells into the gap to cover the scratch was assessed [42].

Formulations CS1-CS6 and a commercial formulation (CollDrez®) were subjected to a scratch assay. L929 murine fibroblast cell lines were seeded onto 12-well plate to a final cell count of 1.2×105 cells/well for the scratch assay. Two millilitres of DMEM-HG media enriched with 10% foetal bovine serum (FBS) was added, and cell cultures were incubated overnight at 37^0C and 5% CO_2 to allow cell adhesion. Fifty millilitres of DMEM media containing 10% (4.7 mL) of foetal bovine serum albumin (FBS) and 0.3 mL of Penicillin–Streptomycin-Neomycin solution was prepared. The sample preparation consisted of mixing 1 mg with 1 mL of the prepared media. Cell culture monolayers were then scratched with a sterile 10 µL tip, after which 2 mL of media was removed from each well to remove floating dead cells. The sample was added (separate concentrations between 10 and 50 µL), and the volume was made up to 2 mL using freshly prepared media. The control group received only fresh medium. Images of the scratched area were recorded at 10× magnification using an inverted phase-contrast microscope (Laben Instruments, BMI-300). Measurements were taken at 0 h (just after scratching cells), 12 h, and 24 h of incubation in a humidified atmosphere (37 ℃, 5% CO_2). By comparing the width of the final gap (24 h) to the width of the initial gap (0 h), the percentage of cell migration was estimated.

In vivo wound healing studies

The wound healing capacity of the scaffolds was assessed using a full-thickness excision wound model on female Wistar rats weighing between 215 and 220 g. All animals were kept in controlled environments with a 12-h light–12-h dark cycle and provided a regular diet of pellets along with unlimited access to water. The dorsal area was depilated and disinfected before wounding. Lignocaine (60 mg/kg) and ketamine hydrochloride (16.5 mg/kg) were administered in combination by the i.p. route to anesthetize the rats. A full-thickness wound measuring 6 mm in diameter was created using a sterile biopsy punch, maintaining uniformity in size and depth. Five groups of rats ($n=6$ in each group) were treated with either a commercial collagen dressing (CollDrez®) or one of three test formulations (CS4, CS5, or CS6) applied daily. The control group was left untreated. Before each dressing change, the wound bed was cleaned with sterile saline to remove debris, blood, and necrotic tissue. The wound area was measured on days 3, 6, 9, 12, and 15 post-wounding, and the % closure was calculated [37].

$$\%\ \text{Wound closure} = \frac{\text{Wound area on day } 0 - \text{Wound area on day } 'n'}{\text{Wound area on day } 0} \times 100$$

where 'n' denotes the day of measurement.

Histopathological analysis

On the 15th day of the study, healed skin samples from anesthetized animals were obtained and stored in 10% formalin. The specimens were then prepared for microscopic evaluation by being fixed in a block of paraffin, sectioned into thin sections (4 µm), and stained with haematoxylin and eosin (H&E) and Masson's trichrome (MT). The staining revealed information about collagen deposition, epithelisation, fibroblast proliferation, and keratinization [43].

Statistical analysis

The statistical analysis of wound contraction data was performed using one-way ANOVA, followed by comparisons with the control group through Dunnett's test. A p-value less than 0.05 was considered statistically significant. GraphPad Prism (V9.4) was used for the statistical analyses.

Results

In this study, nano-calcium sulphate-piscean collagen scaffolds were developed and tested for their ability to promote wound healing. Each batch of formulations contained different amounts of piscean collagen and HPMC E 15 LV, along with 100 ppm NCS. The NCS concentration was fixed on the basis of studies reported earlier [26, 27].

Size and distribution of NCS particles

The average diameter of the NCS particles, as measured by DLS, was 220.7 nm, with a polydispersity index of 0.005 (Fig. 1).

Microscopic analysis and elemental composition by SEM–EDX

SEM–EDX was utilized to analyse the microstructure and ascertain the elemental composition of NCS-loaded scaffolds. The micrograph of the NCS at 50000× magnification revealed the presence of flat, stick-like crystal aggregates (Fig. 2a), and the findings were comparable to SEM data reported in previous studies [44]. The examination of the scaffold at 5000× magnification revealed a porous exterior, while the elemental analysis indicated the presence of peaks corresponding to oxygen, sulphur, and calcium (Fig. 2b, c).

pH

The pH of damaged skin typically changes from basic to neutral pH and then to acidic pH as the wound heals, with complete epithelialization [45–47]. Monitoring the pH of the wound is crucial for healing and can provide insight into the wound's response to treatment. In this study, the pH of the scaffolds was found to be in the range of 5.52 ± 0.01 to 5.61 ± 0.008 (Table 2).

Thickness, folding endurance, and mechanical properties

Wound dressings should be flexible and resistant to rupture during their application or handling. All the formulations exhibited thickness values ranging from 0.54 ± 0.04 to 0.64 ± 0.04 mm, while the folding endurance was between 295 ± 1.20 and 300 ± 0.95. The scaffolds had a smooth texture with good flexibility.

The ability of a dressing to resist stress and pressure during handling or manufacturing was evaluated based on its mechanical characteristics [27, 48]. The tensile strength of the scaffolds was between 2.14 ± 0.19 and 4.59 ± 0.04 N/mm^2. Formulation CS 6, containing 15% collagen and 10% HPMC, exhibited higher thickness and tensile strength when compared to the other formulations (Table 2). Overall, the results indicated that the scaffolds had adequate strength to withstand mechanical stress during handling or application. This can be attributed to the use of collagen and HPMC, which provided

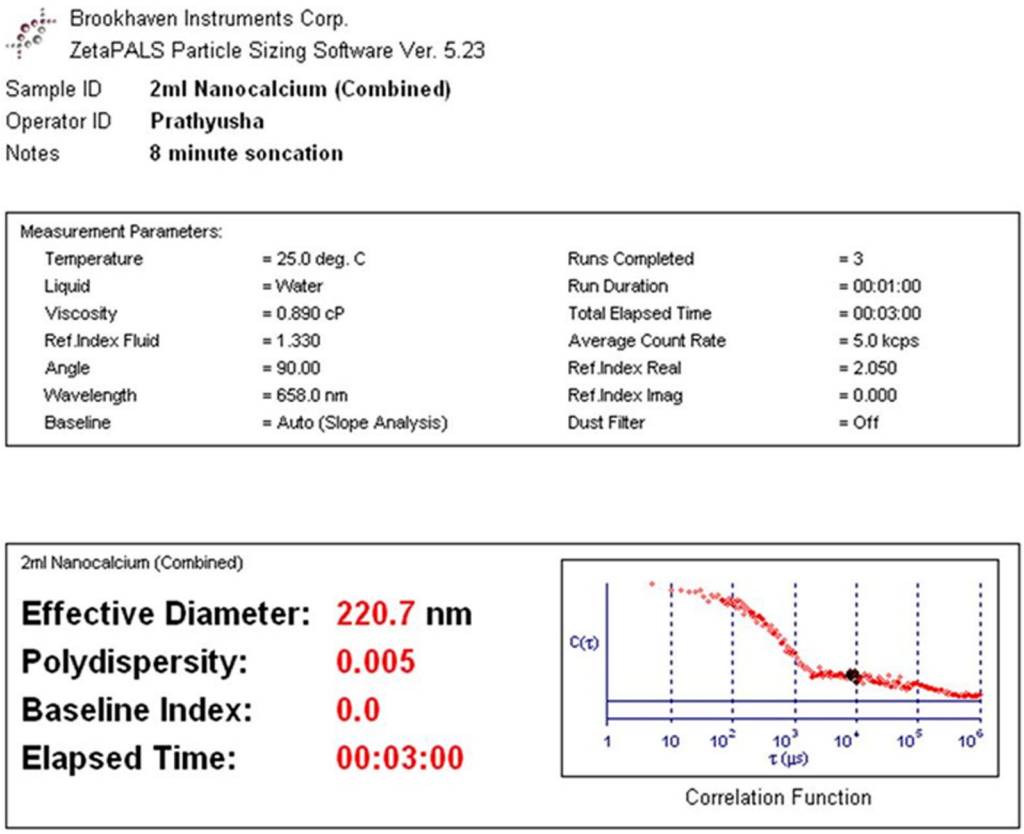

Fig. 1 Size analysis of NCS particles

structural support and improved the integrity of the dressing material.

Moisture vapour transmission rate (MVTR) studies

This study helped to determine the moisture permeability of the scaffolds. Wound dressings must be able to sustain a moist wound milieu. If the MVTR of a dressing is too low, healthy tissues surrounding the wound can undergo maceration and possible infection due to poor drainage of exudates, while a high MVTR can dehydrate the wound surface due to excessive loss of fluid. Data were gathered throughout a 24-h period on the assumption that scaffolds would be applied every day. The MVTR of the scaffolds was calculated to be in the range 1755.72 ± 1.33 to 1925.25 ± 0.81 g/m^2/day (Table 2). A significant increase in MVTR was observed in scaffolds with higher HPMC concentrations.

Expansion profile

When applied to a wound, dressings are expected to absorb wound exudates without any modification in their structural integrity. The expansion of the scaffold in the wound milieu was estimated using solidified gelatin (4% w/v). The percentage expansion of the scaffolds at various time intervals is shown in Fig. 3. During hydration, the scaffolds expanded gradually up to 85–96% of their initial diameter within 20 min. The increased expansion of CS4 (93 ± 2.1), CS5 (94 ± 2.4), and CS6 (96 ± 1.5) could be attributed to the higher concentration of HPMC, a hydrophilic polymer [49–52].

Sterility testing

A direct inoculation technique was employed to test the sterility of the formulations. Following a 14-day post-incubation period, all formulations were found to be free of microbial growth in both culture media (Fluid thioglycollate and Soyabean casein digest medium). In contrast, the positive controls, which had been seeded with *Staphylococcus* aureus and *Candida albicans*, exhibited turbidity (Fig. 4). These results unequivocally demonstrated the sterility of the scaffolds.

Cytocompatibility testing

The results of the cytocompatibility test conducted on formulations CS1–CS6 after 48 h of exposure are shown in Fig. 5. Overall, the % viability of L929 cells in the presence of scaffold formulations (highest concentration of

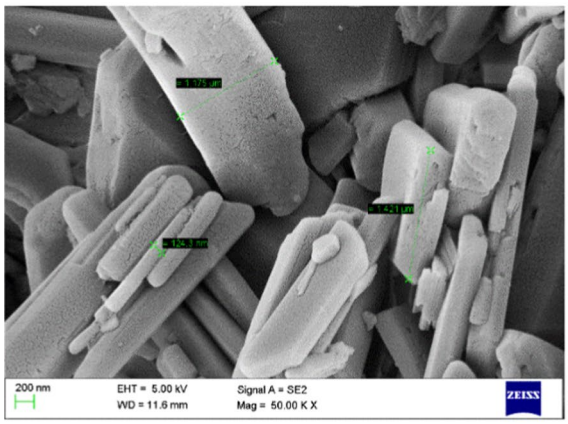

a

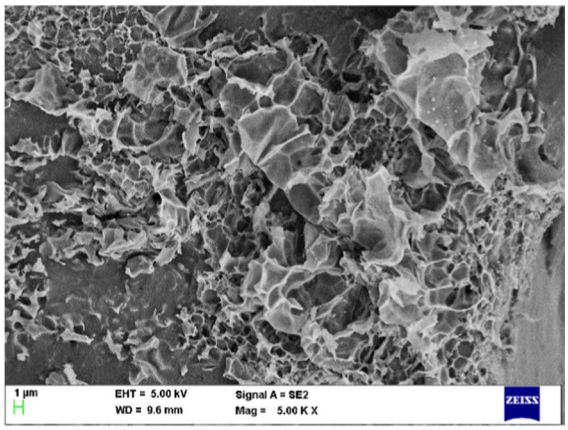

b

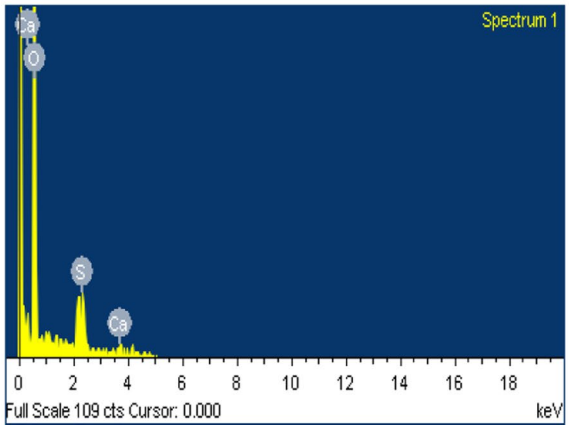

c

Element	Weight%	Atomic%
O K	53.79	72.47
S K	19.96	13.42
Ca K	26.25	14.2

Fig. 2 SEM micrographs of **a** NCS, **b** Scaffold, **c** EDX analysis report of scaffold

Table 2 Evaluation of collagen scaffolds

Parameters #	CS 1	CS 2	CS 3	CS 4	CS 5	CS 6
pH	5.66 ± 0.01	5.59 ± 0.01	5.61 ± 0.008	5.52 ± 0.01	5.53 ± 0.009	5.56 ± 0.004
Thickness(mm)	0.55 ± 0.04	0.54 ± 0.04	0.55 ± 0.04	0.59 ± 0.01	0.63 ± 0.04	0.64 ± 0.04
Folding endurance	295 ± 1.20	296 ± 0.95	299 ± 1.73	299 ± 1.12	300 ± 0.95	300 ± 0.91
Tensile strength (MPa)	2.14 ± 0.19	2.28 ± 0.05	2.33 ± 0.23	2.75 ± 0.05	3.69 ± 0.02	4.59 ± 0.04
Elongation at break (%)	17.96 ± 0.21	19.13 ± 0.21 ^{s}	19.54 ± 0.21	23.07 ± 0.21	30.96 ± 0.21	38.51 ± 0.21
MVTR ($g/m^2/day$)	1755.72 ± 1.33	1776.66 ± 1.02	1780.54 ± 0.94	1890.86 ± 1.34	1905.12 ± 0.58	1925.25 ± 0.81
Expansion Profile (%)	85 ± 2.3	86 ± 1.5	90 ± 2.2	93 ± 2.1	94 ± 2.4	96 ± 1.5

The readings are expressed as mean ± SD ($n = 3$)

2.5% v/v) was found to be in the range 99.89 ± 0.78 of 99.98 ± 0.89.

Acute dermal irritation studies

The results of the dermal irritation studies conducted on rabbits are presented in Fig. 6. The study was conducted using formulation CS6, which had the highest concentration of piscean collagen and HPMC. No adverse dermal responses, such as erythema or oedema, were observed in the rabbits after exposure to the scaffold for 4 h. Additionally, the rabbits did not exhibit any discomfort with the formulations.

In vitro wound healing studies by scratch assay

To ascertain its effects on the migratory activities of fibroblasts, a scratch assay was performed to evaluate the wound healing activity of all formulations. L929 cells were treated with the formulations for 24 h. Cell migration at 0, 12, and 24 h was captured using an inverted phase-contrast microscope, and the distance of wound

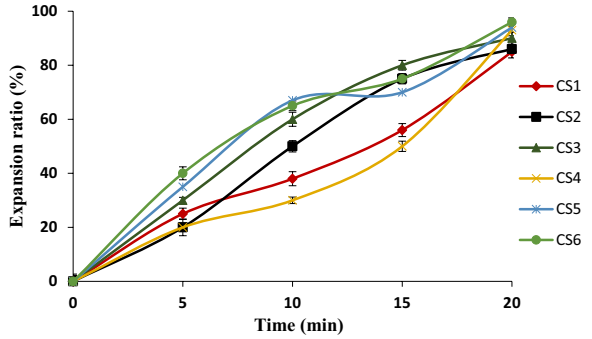

Fig. 3 Expansion profile of collagen scaffolds

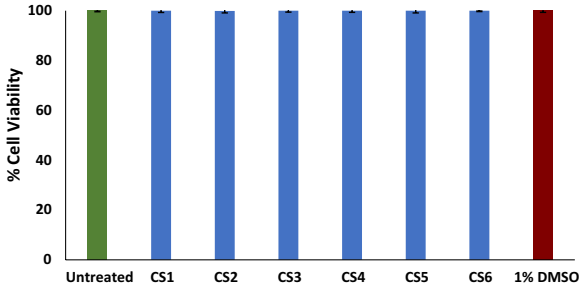

Fig. 5 Viability of L929 cells after 48-h exposure to formulations CS1-CS6 (concentration – 2.5% v/v). Untreated cells were taken as negative control and the vehicle control was 1% DMSO. The values are expressed as mean ± S.D of triplicates

closure was calculated. The findings revealed that at the end of 24 h of the study, there was faster migration and complete closure of the wound gap in formulation administered cells (100%) in contrast to the untreated group (50%). The CollDrez® group showed 91.67% wound closure, and thus, it can be concluded that formulation-treated groups had better healing activity than the control and commercial formulations (Fig. 7).

In vivo wound healing studies

Based on the results obtained from the scratch assay, formulations CS4, CS5, and CS 6 were considered for in vivo studies using an excisional model. Figure 8 depicts the healing effects of the nano-calcium sulphate-incorporated piscean collagen scaffolds at the end of the treatment period. The formulation and CollDrez®-treated wounds underwent contraction and faster re-epithelialization within 12 days post-wounding, while the control group exhibited delayed healing. All rats endured the duration of the study with no evidence of necrosis or inflammation. In comparison with commercial (CollDrez®) and all other formulations, the group treated with CS6 showed the best healing activity overall (100.0 ± 0.05% per cent on day 12) (Table 3).

Histopathology

Re-epithelialization and collagen formation in full-thickness wounds were evaluated using H&E and MT staining, respectively. Microscopic examination of healed skin sections on day 15 (Fig. 9) revealed successful wound healing in all formulations and in CollDrez®-treated animals. The control group revealed the presence of irregular connective tissue, a thinner epidermal layer, and poorly formed collagen fibres (blue arrow) compared to the other groups. Inflammation was also observed, indicating incomplete healing even on day 15. The group treated with CollDrez® dressings revealed a normal epidermal

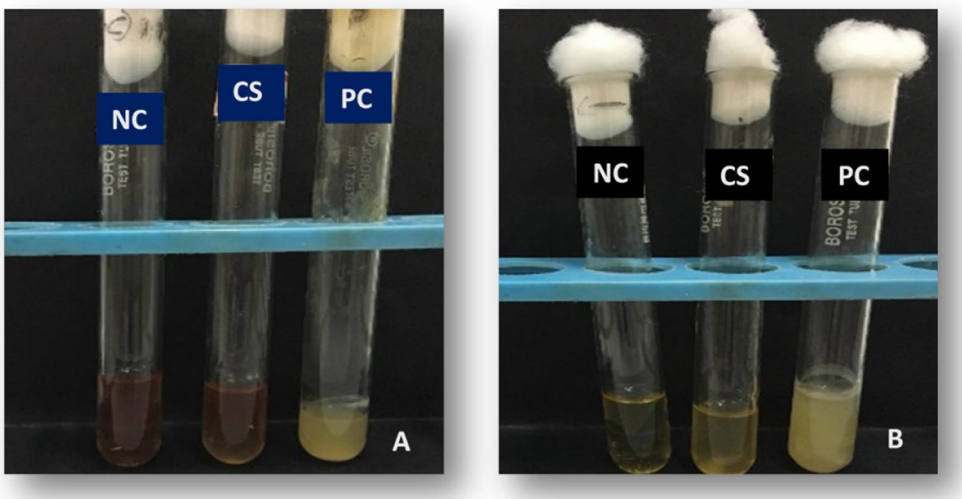

Fig. 4 Sterility testing of scaffolds **a** Testing for bacteria **b** Testing for fungi. *NC* negative control; *CS* collagen scaffold; *PC* positive control

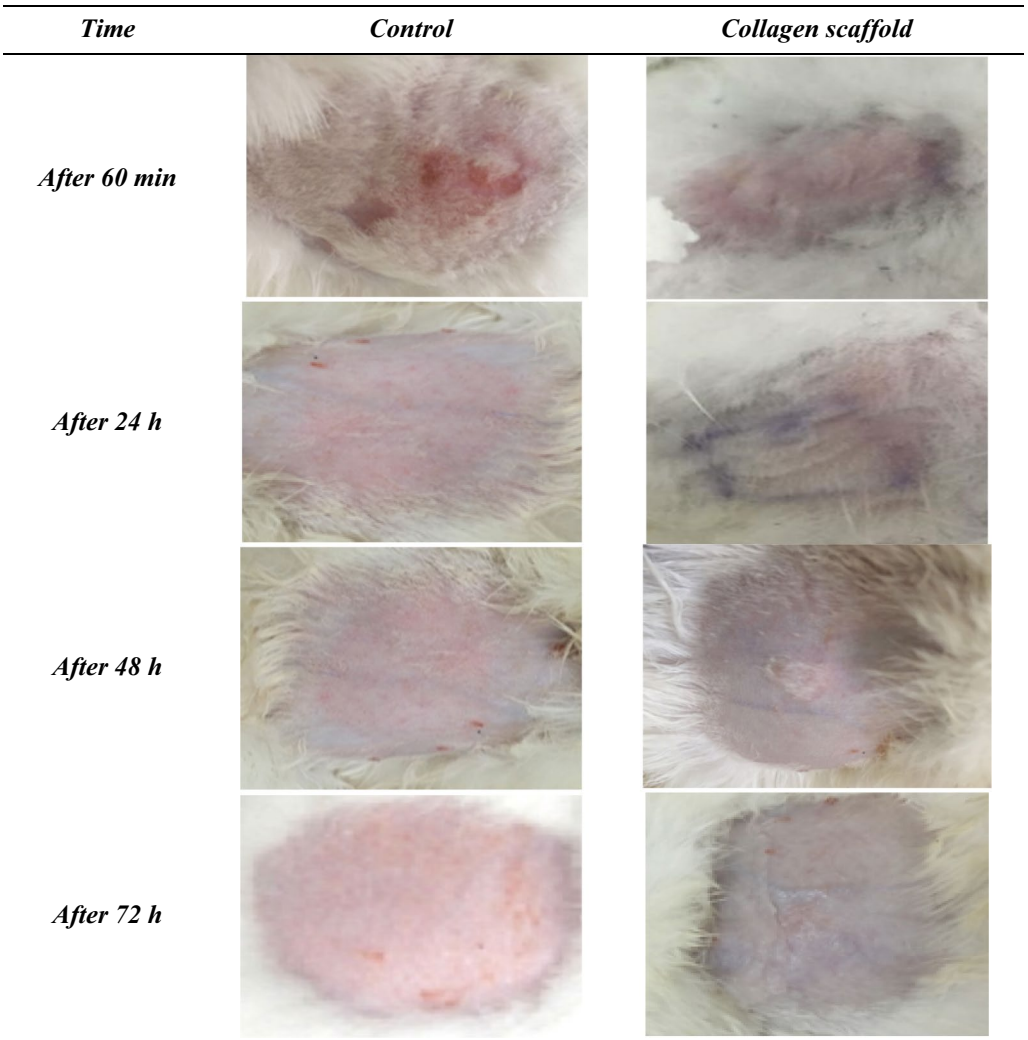

Fig. 6 Photographs of dermal irritation at different time intervals on rabbits

architecture, collagen fibres, and angiogenesis. The thickness of the epidermis was greater than that of the control, but thinner than that of the formulation-treated groups. Groups CS4, CS5, and CS6 showed well-developed epidermal layers with abundant collagen fibres and an absence of inflammatory cells, indicating improved re-epithelialization, fibroblast proliferation, and collagen deposition. The results of the in vivo wound healing experiments were reinforced by the findings from the histological examination.

Discussion

The four main stages of wound healing are haemostasis, inflammatory response, remodelling, and maturation. The type of wound affects the choice of the drug used for tissue repair and its mode of delivery. The choice of dressings is based on factors such as their ability to absorb wound exudates, cost considerations, ease of application or removal, and their potential to accelerate the healing process. In the present study, nano-calcium-incorporated piscean collagen scaffolds were developed and investigated for their potential as a wound dressing material [53]. The scaffolds were embedded with nano-calcium sulphate of average diameter of 220.7 nm. The porosity of a scaffold is crucial to provide appropriate areas for cell accommodation, proliferation, migration, and differentiation. Through the 3D matrix, porous scaffolds also aid in the oxygenation and nourishment of the injured skin [54, 55]. SEM–EDX examination of the scaffold revealed the presence of a porous exterior, which would be beneficial for maintaining an ideal wound microenvironment for quicker epithelialization [22]. pH is a major factor in determining the prognosis of wound healing, and the pH measurements were found to be in agreement with other studies that have demonstrated that lower pH promotes re-epithelialization and reduces

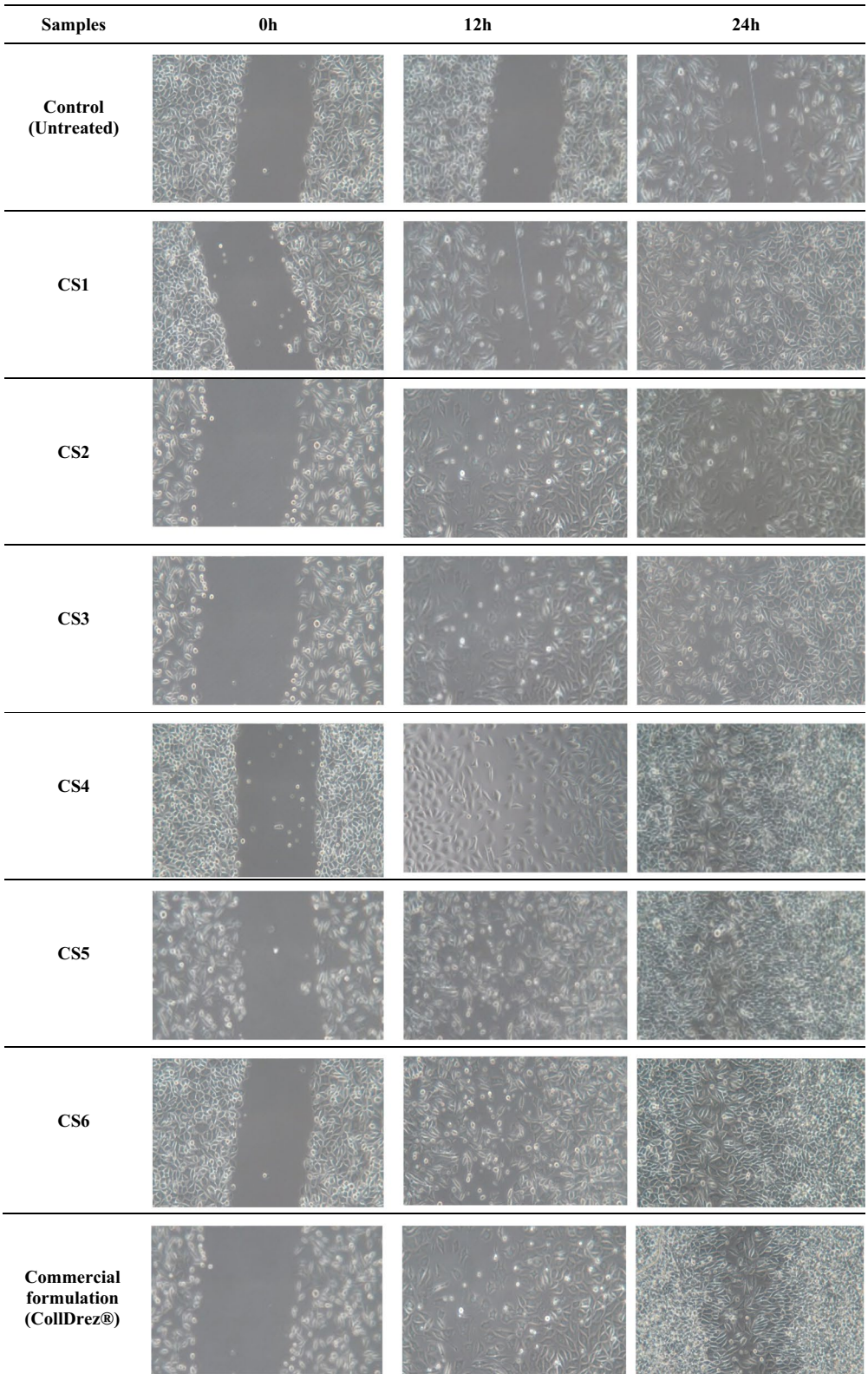

Fig. 7 Scratch assay using L929 murine fibroblast cell lines

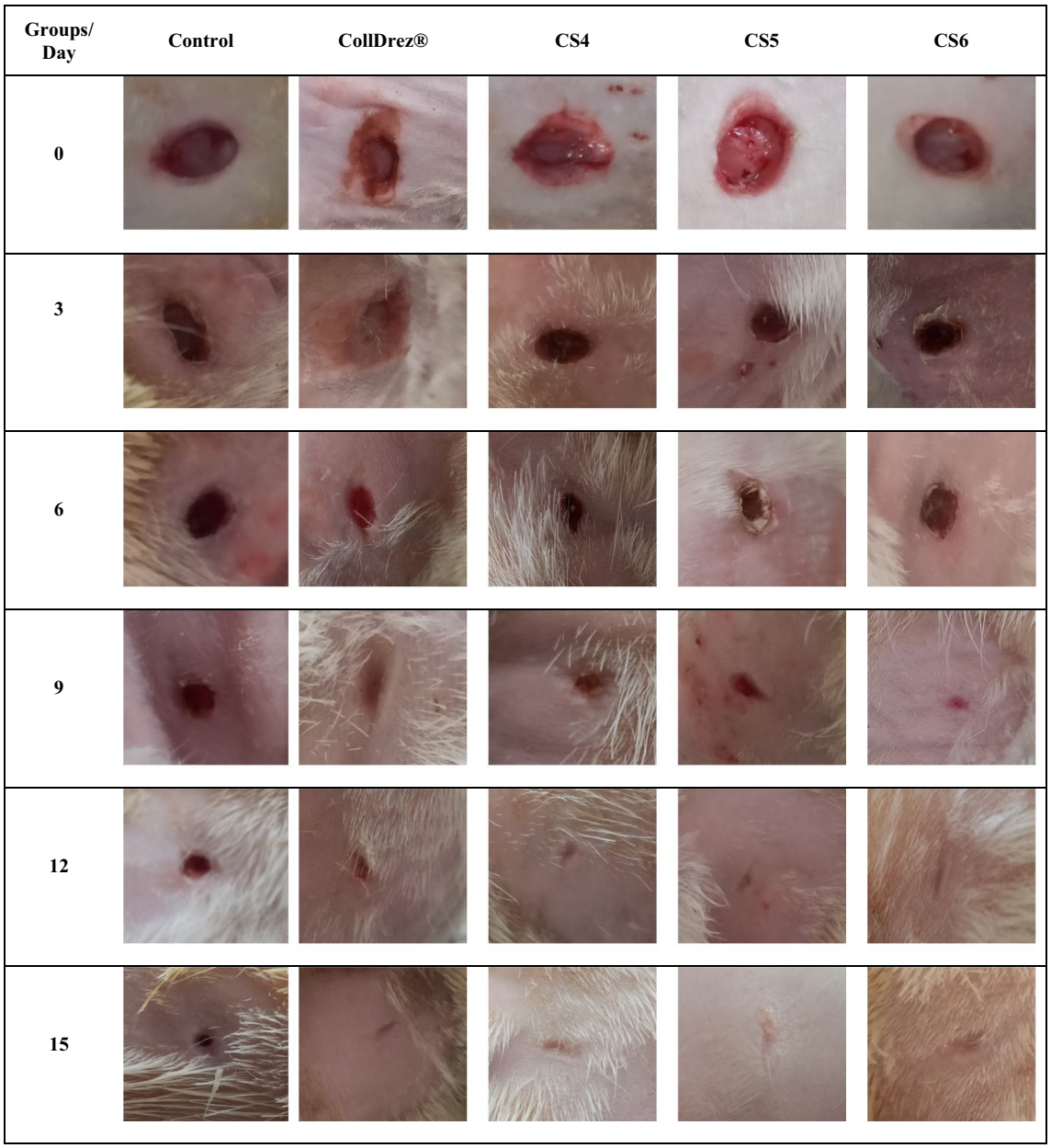

Fig. 8 Representative images of wound control and wounds treated with CollDrez® and test formulations for 15 days. The scale bar for all images is 5 mm

Table 3 Data for statistical analysis of wound healing activity

Group	Control	CollDrez®	CS4	CS5	CS6
Day 3	12.00 ± 0.98	13.00 ± 0.82 ^{ns}	13.00 ± 0.81 ^{ns}	15.00 ± 0.81*	17.00 ± 0.50**
Day 6	19.00 ± 0.81	40.00 ± 0.60**	41.00 ± 0.59**	45.00 ± 0.55**	49.00 ± 0.51**
Day 9	35.00 ± 0.65	64.90 ± 0.35**	76.00 ± 0.24**	79.00 ± 0.21**	85.00 ± 0.15**
Day 12	68.00 ± 0.32	74.00 ± 0.26**	80.00 ± 0.20 **	88.00 ± 0.15**	100.0 ± 0.05**
Day 15	75.00 ± 0.25	93.00 ± 0.10**	90.00 ± 0.10**	99.50 ± 0.04**	–

The readings are expressed in terms of %, as Mean ± S.D ($n = 6$); one-way ANOVA and Dunnett test where ns—(non-significant) $p > 0.05$, *$p < 0.05$, **$p < 0.01$, in comparison with control

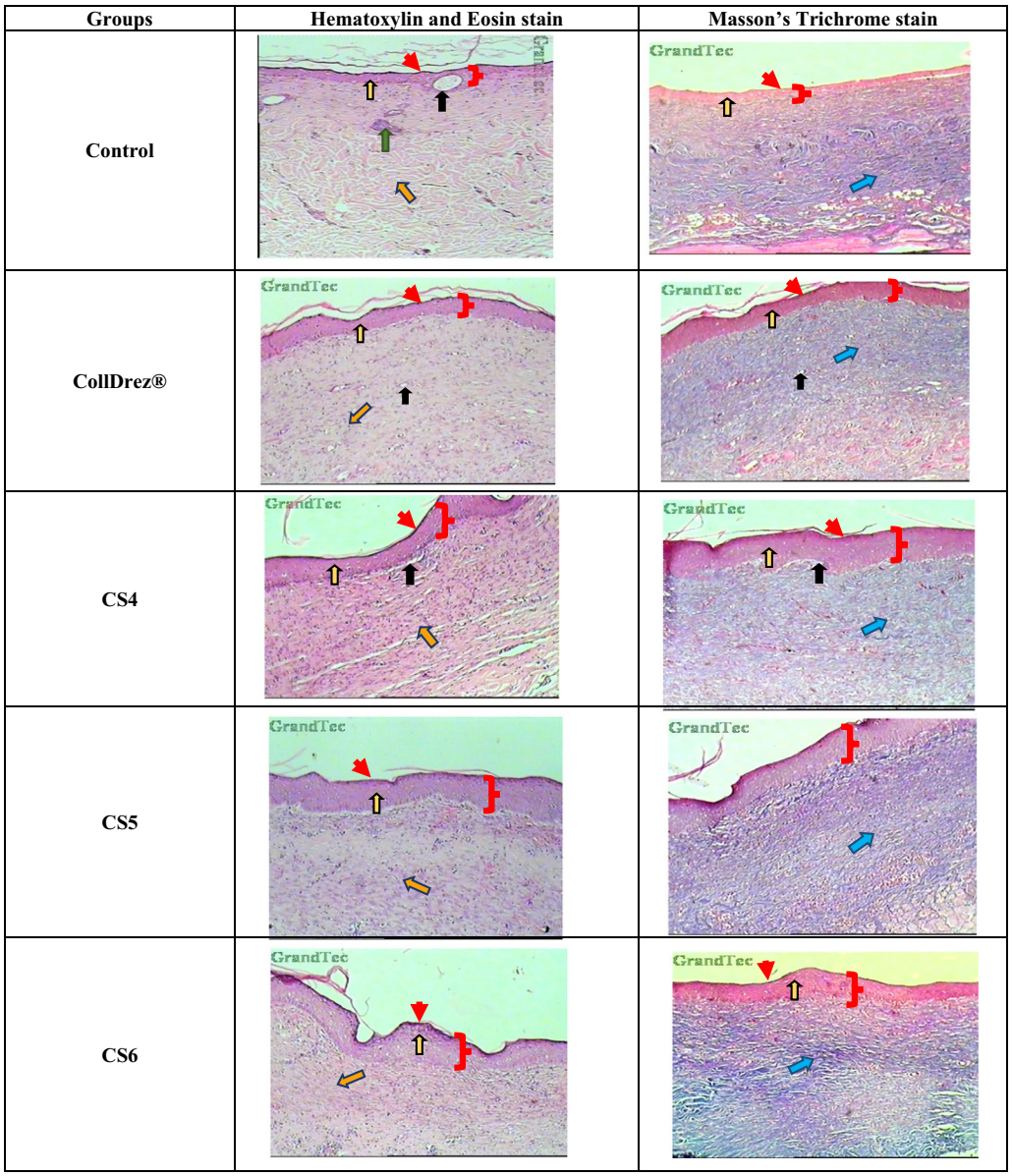

Fig. 9 Photomicrographs showing stained sections of skin tissues of different groups, at 10x magnification. The scale bar for all images is 100 µm. The areas are indicated by coloured arrows—Red: Re-epithelialization; Black: Irregular connective tissues; Yellow: Epidermis; Green: Inflammatory cells; Blue: Collagen formation; Orange: blood vessels; and the red bracket representing the thickness of the epithelial layer

microbial load on infected surfaces [56–58]. All wound dressings should possess apt mechanical properties to accommodate different types of skin wounds. Additionally, they should be flexible and resistant to rupture during their application or handling [59]. The scaffolds had a smooth texture devoid of irregularities, good flexibility and adequate strength to withstand mechanical stress during handling and application, according to the evaluation results of their mechanical characteristics [27, 48]. The study also concluded that the tensile strength of the formulations could be improved by incorporating higher concentrations of collagen and HPMC. According to previous studies, an MVTR of approximately 2028.3 g/m^2/day is ideal for maintaining moist conditions in the wound without increasing the risk of maceration or dehydration [60]. The results indicated that all the scaffolds were pervious to water vapour and could sustain an optimum milieu on the wounded area without leading to desiccation. Water uptake capacity is considered to be a prerequisite for polymers selected in the development of wound dressing materials, and dressings with good hydration properties are ideal for wounds with low

or moderate discharge [61–63]. During hydration, the scaffolds expanded gradually up to 85–96% of their initial diameter while maintaining their shape throughout the test. Expansion was pronounced with the increase in concentration of HPMC, owing to its hydrophilic nature [64].

In accordance with Fouche et al. [65], a substance is deemed non-cytotoxic when the cell viability is 80% or higher, weakly cytotoxic when the cell viability is 60–80%, moderately cytotoxic when the cell viability is 40–60%, and strongly cytotoxic when it is less than 40%. Thus, the scaffolds can be considered safe for dermal application, as they do not have any cytotoxic effects on mouse fibroblasts in vitro. No visible dermal responses, such as erythema or oedema, were observed on the rabbits following exposure to the scaffold for 4 h in the acute dermal irritation studies, and the rabbits did not show any kind of discomfort with the formulations. The findings of the scratch assay showed that the formulation-treated groups had better healing activity than the control and commercial formulations, as there was faster migration and complete closure of the wound gap in formulation-administered cells at the end of 24 h of the study, in contrast to the untreated and commercial formulation-treated groups. The results of the scratch assay were further substantiated by in vivo wound-healing experiments and histological studies. These outcomes are consistent with previous research that showed that formulations containing nano-calcium enhanced wound healing and epidermal regeneration [27, 43]. Additionally, the presence of collagen and HPMC's effective exudate-absorbing capabilities of HPMC can be considered as additional factors responsible for healing [66].

Conclusion

In the present study, we propose the development of nano-calcium-integrated piscean collagen scaffolds as a potential material for wound dressings. The scaffolds exhibited good mechanical characteristics and were compatible with dermatology. Significant cell proliferation was observed in the scratch assay performed using L929 mouse fibroblasts. The dual wound healing benefits of both piscean collagen and nano-calcium were evident for all formulations. The authors concluded that the nano-calcium-incorporated piscean collagen scaffold is a promising biomaterial that can be further explored in wound treatment.

Further investigations can be carried out to optimize the concentrations of various polymers and consider factors such as nutrition and comorbidities in animals to create a more comprehensive model for simulating real-world wound healing conditions.

Abbreviations

CS	Collagen scaffold
DMSO	Dimethyl sulfoxide
DMEM-HG	Dulbecco's modified Eagle medium with high glucose
FBS	Foetal bovine serum
H&E	Haematoxylin and eosin
HPMC	Hydroxypropyl methylcellulose
i.p	Intraperitoneal
MVTR	Moisture vapour transmission rate
MT	Masson's trichrome
NCS	Nano-calcium sulphate
NC	Negative control
PC	Positive control
SEM–EDX	Scanning electron microscopy and energy-dispersive X-ray spectroscopy
S.D	Standard deviation
TS	Tensile strength

Acknowledgements

The authors extend their gratitude to MSRUAS for providing necessary facilities to support this project. They also thank Micro and Nano Characterization Facility (MNCF), Centre for Nano Science and Engineering (CeNSE), Indian Institute of Science, Bengaluru for their assistance in conducting ZetaPALS and SEM-EDX studies by providing instrumentation facilities.

Author contributions

All authors contributed to the study's conception and design. The project was conceptualized and initiated by SA. CS, DR, KD and SF carried out material preparation, data collection, and analysis. The manuscript was written by SA, reviewed and edited by BS. All authors have read and approved the final manuscript.

Funding

This research has not received external funding.

Availability of data and materials

All data generated during this study are available as a part of this article and no additional source data are required.

Declarations

Ethics approval and consent to participate

The animals were obtained from the in-house animal house facility, Department of Pharmacology, Faculty of Pharmacy, and the protocol was approved by the Institutional Animal Ethical Committee (IAEC), vide reference number XXII/MSRFPH/CEU/M-07; 24.09.2019.

Consent for publication

We certify this manuscript has not been published elsewhere and is not submitted to another journal. All authors have approved the manuscript and agreed to submit it to Future Journal of Pharmaceutical Sciences.

Competing interests

The authors declare that they have no competing interests.

Received: 18 October 2023 Accepted: 1 December 2023
Published online: 21 December 2023

References

1. Kawai K, Larson BJ, Ishise H, Carre AL, Nishimoto S, Longaker M, Lorenz HP (2011) Calcium-based nanoparticles accelerate skin wound healing. PLoS ONE 6:27106
2. Kamolz LP, Griffith M, Finnerty C, Kasper C (2015) Skin regeneration, repair, and reconstruction. BioMed Res Int 892031
3. Park HEJ, Foster DS, Longaker MT (2018) Fibroblasts and wound healing: an update. Regen Med 13:491–495

4. Sinha M (2018) Advance measures and challenges of wound healing. J Pharmacol Ther Res 2:1–3
5. Deepa T, Megha S, Neethu M, Reshmy R, Eapen P, Latha MS (2020) Alginate film modified with aloe vera gel and cellulose nanocrystals for wound dressing application: preparation, characterization, and *in vitro* evaluation. J Drug Deliv Sci Technol 59:101894
6. Rangaraj A, Harding K, Leaper D (2011) Role of collagen in wound management. Wounds UK 7:54–63
7. Singh O, Gupta SS, Soni M, Moses S, Shukla S, Mathur RK (2011) Collagen dressing versus conventional dressings in burn and chronic wounds: a retrospective study. J Cutan Aesthet Surg 4:12–16
8. Ilenghoven D, Chan CY, Kamal WWA, Mohd Yussof SJ, Ibrahim SA (2017) Review of wound dressing practices. Clin Dermatol J 2:000133
9. Rodriguez MIA, Barroso LGR, Sanchez ML (2018) Collagen: a review on its sources and potential cosmetic applications. J Cosmet Dermatol 17:20–26
10. Mehta MA, Shah S, Ranjan V, Sarwade P, Philipose A (2015) Comparative study of silver-sulfadiazine-impregnated collagen dressing versus conventional burn dressings in second-degree burns. J Fam Med Prim Care 8:215–219
11. Rodriguez F, Moran L, Gonzalez G, Troncoso E, Zuniga RN (2017) Collagen extraction from mussel byssus: a new piscean collagen source with physicochemical properties of industrial interest. J Food Sci Technol 54:1228–1238
12. Chen J, Gao K, Liu S, Wang S, Elango J, Bao B, Dong J, Liu N (2019) Fish collagen surgical compress repairing characteristics on the wound healing process in vivo. Mar Drugs 17:33
13. Coppola D, Oliviero M, Vitale GA, Lauritano C, D'Ambra I, Iannace S, Pascale D (2020) Marine collagen from alternative and sustainable sources: extraction, processing and applications. Mar Drugs 18:214
14. Cruz MA, Araujo TA, Avanzi IR, Parisi JR, de Andrade ALM, Renno ACM (2021) Collagen from marine sources and skin wound healing in animal experimental studies: a systematic review. Mar Biotechnol 23:1–11
15. De Souza A, de Almeida Cruz M, de Araujo TAT, Parisi JR, do Vale GCA, Dos Santos Jorge Sousa K, Ribeiro DA, Granito RN, Renno ACM (2022) Fish collagen for skin wound healing: a systematic review in experimental animal studies. Cell Tissue Res 388:489–502
16. Huang JS, Mukherjee JJ, Chung T, Crilly KS, Kiss Z (1999) Extracellular calcium stimulates DNA synthesis in synergism with zinc, insulin, and insulin-like growth factor I in fibroblasts. Eur J Biochem 266:943–951
17. Pervin MS, Itoh G, Talukder MS, Fujimoto K, Morimoto YV, Tanaka M et al (2018) A study of wound repair in dictyostelium cells by using novel laserporation. Sci Rep 8:7969
18. Hampton S (2004) The role of alginate dressings in wound healing. Diabet Foot 7(4):162–167
19. Pecora G, De Leonardis D, Ibrahim N, Bovi M, Cornelini R (2001) The use of calcium sulfate in the surgical treatment of a 'through and through' periradicular lesion. Int Endod J 34:189–197
20. Budhiraja S, Bhavsar N, Kumar S, Desai K, Duseja S (2012) Evaluation of calcium sulfate barrier to collagen membrane in intrabony defects. J Periodontal Implant Sci 42:237–242
21. Turri A, Dahlin C (2015) Comparative maxillary bone-defect healing by calcium sulfate or deproteinized bovine bone particles and extracellular matrix membranes in a guided bone regeneration setting: an experimental study in rabbits. Clin Oral Implants Res 26:501–506
22. Laurel T, Karmon MP, Nguyen D, Dziak R (2017) Nano calcium sulfate and collagen biomaterials: effects on osteoblastic cells. Dent Oral Craniofac Res 3:1–5
23. Fernandes G, Abhyankar V, Josanne MOD (2021) Calcium sulfate as a scaffold for bone tissue engineering: a descriptive review. J Dent Oral Disord Ther 9:1–22
24. Walsh WR, Morberg P, Yu Y, Yang JL, Haggard W, Sheath PC, Svehla M, Bruce WJ (2003) Response of a calcium sulfate bone graft substitute in a confined cancellous defect. Clin Orthop Relat Res 406:228–236
25. Park YB, Mohan K, Al-Sanousi A, Almaghrabi B, Genco RJ, Swihart MT, Dziak R (2011) Synthesis and characterization of nanocrystalline calcium sulfate for use in osseous regeneration. Biomed Mater 6:055007
26. Vemuri S, Abraham S, Azamthulla M, Furtado S, Srinivasan B (2020) Development of in situ gels of nano calcium oxide for healing of burns. Wound Med 28:100177
27. Abraham S, Harsha GGS, Desai K, Furtado S, Srinivasan B (2022) Nano calcium oxide incorporated hydrocolloid dressings for wound care. J Pharm Innov 17:215–226
28. Wight TN, Merrilees MJ (2004) Proteoglycans in atherosclerosis and restenosis: key roles for versican. Circ Res 94(9):1158–1167
29. Dang Q, Liu K, Zhang Z, Liu C, Liu X, Xin Y et al (2017) Fabrication and evaluation of thermosensitive chitosan/collagen/alpha, beta-glycerophosphate hydrogels for tissue regeneration. Carbohydr Polym 167:145–157
30. Wang Z, Hu S, Wang H (2017) Scale-up preparation and characterization of collagen/sodium alginate blend films. J Food Qual 4954259
31. James CYD, Chan WY, Cristini V, Kim JS, Lowengrub J, Singh S, Benjamin MW (2006) Analysis of cell growth in three-dimensional scaffolds. Tissue Eng 12:705–716
32. Arora R, Aggarwal G, Harikumar SL, Kaur K (2014) Nanoemulsion based hydrogel for enhanced transdermal delivery of ketoprofen. Adv Pharm 468456
33. Kulkarni S (2019) Formulation and evaluation of transdermal patch for atomoxetine hydrochloride. J Drug Deliv Ther 9:32–35
34. ASTM D882-18 (2018) Standard test method for tensile properties of thin plastic sheeting. ASTM International, West Conshohocken. www.astm.org. Accessed 4 Jan 2020
35. Rezvanian M, Amin MCIN, Shiow F (2016) Development and physicochemical characterization of alginate composite film loaded with simvastatin as a potential wound dressing. Carbohydr Polym 137:295–304
36. ASTM E96/E96M-16 (2016) Standard test methods for water vapor transmission of materials. ASTM International, West Conshohocken. www.astm.org. Accessed 4 Jan 2020
37. Dolete G, Tihauan BM, Tutunaru O, Mocanu IC, Balas C, Lavinia I et al (2019) Development and sequential analysis of a collagen-chitosan wound management biomaterial. Rom Biotechnol Lett 2:108–117
38. Hu Z, Yang P, Zhou C, Li S, Hong P (2017) Marine collagen peptides from the skin of Nile Tilapia (*Oreochromis niloticus*): characterization and wound healing evaluation. Mar Drugs 15:102
39. Shearer H, Ellis MJ, Perera SP, Chaudhuri JB (2006) Effects of common sterilization methods on the structure and properties of poly (D, L lactic-co-glycolic acid) scaffolds. Tissue Eng 12:2717–2727
40. Liang CC, Park A, Guan JL (2007) In vitro scratch assay: a convenient and inexpensive method for analysis of cell migration in vitro. Nat Protoc 2:329–333
41. OECD (2015) Test No. 404: acute dermal irritation/corrosion, OECD guidelines for the testing of chemicals, Section 4, OECD Publishing, Paris. https://doi.org/10.1787/9789264242678-en.
42. Martinotti S, Ranzato E (2020) Scratch wound healing assay. Methods Mol Biol 2109:225
43. Suvik A, Effendy AWM (2012) The use of modified Masson's trichrome staining in collagen evaluation in wound healing study. Malays J Vet Res 3:39–47
44. Suharso S, Buhani B, Aprilia L (2014) Influence of calix [4] arene derived compound on calcium sulphate scale formation. Asian J Chem 26:6155–6158
45. Leveen HH, Falk G, Borek B, Diaz C, Lynfield Y, Wynkoop B et al (1973) Chemical acidification of wounds: an adjuvant to healing and the unfavorable action of alkalinity and ammonia. Ann Surg 178:745–753
46. Schneider LA, Korber A, Grabbe S, Dissemond J (2007) Influence of pH on wound-healing: a new perspective for wound-therapy. Arch Dermatol Res 298(9):413–420
47. Moen I, Ugland H, Stromberg N, Sjostrom E, Karlson A, Ringstad L et al (2018) Development of a novel in situ gelling skin dressing: delivering high levels of dissolved oxygen at pH 5.5. Health Sci Rep 1:e57
48. Balaure PC, Holban AM, Grumezescu AM, Mogosanu GD, Balseanu TA, Stan MS et al (2019) In vitro and in vivo studies of novel fabricated bioactive dressings based on collagen and zinc oxide 3D scaffolds. Int J Pharm 557:199–207
49. Devi N, Dutta J (2017) Preparation and characterization of chitosan-bentonite nanocomposite films for wound healing application. Int J Biol Macromol 104:1897–1904
50. Putri N, Prihartini W, Djoni IR (2019) Effect of collagen-chitosan-glycerol composition in scaffold for gingival recession therapy. J Biomim Biomater Biomed Eng 40:101–108

51. Yufei S, Hongjian Z, Xin Z, Zhan C, Dan Z, Jun MA (2020) Comparative study of two porous sponge scaffolds prepared by collagen derived from porcine skin and fish scales as burn wound dressings in a rabbit model. Reg Biomat 1:63–70
52. Ndlovu SP, Ngece K, Alven S, Aderibigbe BA (2021) Gelatin based hybrid scaffolds: promising wound dressings. Polymers 13:2959–2990
53. Piraino F, Selimovic S (2015) A current view of functional biomaterials for wound care, molecular and cellular therapies. BioMed Res Int 403801
54. Nosrati H, Aramideh Khouy R, Nosrati A, Khodaei M, Banitalebi-Dehkordi M, Ashrafi-Dehkordi K et al (2021) Nanocomposite scaffolds for accelerating chronic wound healing by enhancing angiogenesis. J Nanobiotech 19(1):1
55. Bainbridge P, Browning P, Bernatchez SF, Blaser C, Hitschmann G (2023) Comparing test methods for moisture-vapor transmission rate (MVTR) for vascular access transparent semipermeable dressings. J Vasc Access 24(5):1000–1007
56. Gethin G (2007) The significance of surface pH in chronic wounds. Wounds UK 3:52–56
57. Sharpe JR, Booth S, Jubin K, Jordan NR, Lawrence Watt DJ, Dheansa BS (2013) Progression of wound pH during the course of healing in burns. J Burn Care Res 3:e201–e208
58. Ono S, Imi R, Ida Y, Shibata D, Komiya T, Matsumura H (2015) Increased wound pH as an indicator of local wound infection in second-degree burns. Burns 41:820–824
59. Negut I, Dorcioman G, Grumezescu V (2010) Scaffolds for wound healing applications. Polymers 12(9):2010
60. Xu R, Xia H, He W et al (2016) Controlled water vapor transmission rate promotes wound healing via wound re-epithelialization and contraction enhancement. Sci Rep 6:24596
61. Kandra R, Bajpai S (2021) Wound dressing application of Ch/CD nanocomposite film. In: Chitin and chitosan—physicochemical properties and industrial applications. IntechOpen. Available from: https://doi.org/10.5772/intechopen.95107
62. Alruwaili NK et al (2022) Arabinoxylan-carboxymethylcellulose composite films for antibiotic delivery to infected wounds. Polymers 14:1769
63. Alzarea AI et al (2022) Development and characterization of gentamicin-loaded arabinoxylan-sodium alginate films as antibacterial wound dressing. Int J Mol Sci 23(5):2899
64. Ghadermazi R, Hamdipour S, Sadeghi K, Ghadermazi R, Khosrowshahi Asl A (2019) Effect of various additives on the properties of the films and coatings derived from hydroxypropyl methylcellulose-a review. Food Sci Nutr 7(11):3363–3377
65. Fouche M, Willers C, Hamman S, Malherbe C, Steenekamp J (2020) Wound healing effects of aloe muth-muth: in vitro investigations using immortalized human keratinocytes (HaCaT). Biology 9:350–360
66. Tudoroiu EE, Dinu Pirvu CE, Albu Kaya MG, Popa L, Anuta V, Prisada RM, Ghica MV (2021) An overview of cellulose derivatives-based dressings for wound-healing management. Pharmaceuticals 14:1215

Publisher's Note